scientific reports

OPEN

Progressive T cell exhaustion and predominance of aging tissue associated macrophages with advancing disease stage in penile squamous cell carcinoma

Hiroko Miyagi[1,9]✉, Xiaoqing Yu[2,9], Taylor Peak[3], Jasreman Dhillon[4], Casey Le[1], Xuefeng Wang[2], Sean Yoder[5], Doug Marchion[6], Xin Lu[7], Curtis Pettaway[8], Carlos Moran Segura[4], Chaomei Zhang[5], Gabriel Roman Souza[1], Alice Yu[1], Logan Zemp[1], Philippe Spiess[1,9] & Jad Chahoud[1,9]✉

Penile squamous cell carcinoma (PSCC) is a rare malignancy with limited understanding of the tumor immune microenvironment (TIME). The interplay between PSCC and the immune system across disease progression and HPV infection status remains poorly characterized. This study aims to assess the TIME changes from localized to advanced disease and between HPV-positive versus negative tumors to identify potential immune evasion mechanisms in advanced PSCC. scRNA-seq was performed on ten PSCC tissue samples from penile, lymph node and distant metastatic sites with four matched penile and lymph node samples to understand the cellular heterogeneity within PSCC tumors. Analysis of immune cell populations and transcriptional hallmarks were performed stratified by localized (pT1–3, N0) versus advanced (N1–3, M0 or any N, M1) disease states and HPV infection status. We observed significant differences in immune cell infiltration between localized and advanced PSCC disease states and by HPV status. Advanced disease states demonstrated an exhausted immune phenotype, characterized by terminally exhausted CD8+ T cells, M2-like macrophages and hypoxic signature, while localized disease states demonstrated an active innate immune system characterized by increased DCs. HPV-negative tumors displayed low immune cell infiltration while HPV-positive tumors demonstrated an immune exhausted phenotype. These findings offer valuable insights into the evolving PSCC immune landscape, paving the way for the development of potential therapeutic approaches for advanced PSCC.

Abbreviations

PSCC	Penile squamous cell carcinoma
HPV	Human papillomavirus
scRNA-seq	Single cell RNA sequencing
TIME	Tumor immune microenvironment
TME	Tumor microenvironment

[1]Genitourinary Oncology Department, H. Lee Moffitt Cancer Center, 12902 Magnolia Dr, Tampa, FL 33612, USA. [2]Department of Biostatistics and Bioinformatics, H. Lee Moffitt Cancer Center, Tampa, FL 33612, USA. [3]Department of Urology, University of Tennessee College of Medicine, Chatanooga, USA. [4]Pathology Department, H. Lee Moffitt Cancer Center, Tampa, FL 33612, USA. [5]Molecular Genomics Core, H. Lee Moffitt Cancer Center and Research Institute, Tampa, FL, USA. [6]Tissue Core Shared Resource, H. Lee Moffitt Cancer Center and Research Institute, Tampa, FL, USA. [7]Department of Biological Sciences, University of Notre Dame, Norte Dame, IN 46556, USA. [8]Department of Urology, University of Texas MD Anderson Cancer Center, Houston, TX 77030, USA. [9]Hiroko Miyagi, Xiaoqing Yu, Philippe Spiess and Jad Chahoud have contributed equally to this work. ✉email: Hiroko.miyagi@moffitt.org; Jad.chahoud@moffitt.org

mIF	Multiplex immunofluorescence
GSEA	Gene set enrichment analysis
Tregs	Regulatory T cells
Texh	Exhausted T cells
Tn	Naïve T cells
DC	Dendritic cells
TAM	Tumor associated macrophages
TILs	Tumor infiltrating lymphocytes
ICB	Immune checkpoint blockade

Penile squamous cell carcinoma (PSCC) is a rare malignancy that accounts for <1% of cancer in men. In the United States, an estimated 2100 new cases of PSCC are expected to be diagnosed in 2024, with approximately 500 associated deaths. Globally it affects more than 37,000 yearly with around 14,000 associated deaths[1]. Approximately half (50.8%) of PSCC cases are human papillomavirus (HPV) associated and most prior translational research has been only focused on the divergent biology of HPV associated in comparison to HPV negative PSCC[2–4]. An in depth understanding of the interactions between tumor cells and their immune microenvironment is critical to the development of therapeutic approaches for the treatment of PSCC. Over the past 5 years we have witnessed efforts to characterize the PSCC tumor immune miroenvironment (TIME) using bulk transcriptomic or multiplex panel of protein markers to expand our understanding of how the immune composition may impact outcomes in PSCC but were limited by their ability to completely characterize heterogenous immune cells and their different phenotypic states within the tumor microenvironment (TME)[2,5,6].

A detailed characterization of the composition and cellular states of the tumor infiltrating immune cells is critical in expanding our understanding of cancer progression and response to immune based therapy[7]. Single-cell RNA sequencing (scRNA-seq) provides the capacity for comprehensive parallel characterizations of cellular composition and transcriptional states, and has already yielded important insights into the cell-of-origin in PSCC with the landmark study by Elst et al.[8] as the first scRNA-seq PSCC atlas and unveiling TP53 mutations as a key determinant of aggressive phenotypes, irrespective of HPV status[9]. An additional pivotal aspect focusing on the changes in the immune cell populations that occur with advancing disease have not been well characterized in PSCC, limited by a lack of tumor samples from lymph node or visceral metastatic sites[10]. Single-cell transcriptomic studies in other cancers have revealed not only the important role of CD8+ T cells within the TME[11–13] but also that of effector T regulatory cells and myeloid subsets, including tumor-associated macrophages (TAMs)[14,15].

In this study we aim to characterize the different immune cell populations across PSCC stages and HPV status including their transcriptional states and cellular compositions using scRNA-seq. This study provides a detailed view of immune cell evolution across advancing PSCC stages and HPV status, setting the stage for future research opportunities to explore immune evasion mechanisms and potential therapeutic targets for PSCC.

Methods
Detailed methods can be found in the Supplementary material.

Patients and tissue collection
Sixteen fresh tissue samples were collected from biopsy proven PSCC patients of which ten samples passed quality control for scRNA-seq. Tumor samples spanned stages pT1–pT3, pN0–N3, and M0–M1 including five penile specimens, four lymph node metastases, and one metastatic site, with two paired matched tumor samples from separate sites. Human specimen collection was approved by the Moffitt Cancer Center Institutional Review Board and all research procedures were conducted in accordance with the Declaration of Helsinki. Written informed consent was obtained from all participants prior to tissue collection under the total cancer care (TCC) protocol.

HPV status
High-risk HPV in situ hybridization assay (HPV-ISH) was used in combination with p16 immunohistochemistry to determine the HPV status.

Single-cell RNA sequencing and data analysis
Single-cell RNAseq data were processed by Cell Ranger (v7.1.0, 10X Genomics) and analyzed by Seurat V4. Quality filters were applied to remove cells with less than 200 genes detected, cells with lower complexity libraries (in which log10(genes per UMI) < 0.8), cells with greater than 15% mitochondrial UMIs, or doublet cells. Filtered data were further normalized and integrated to remove batch effects. Clustering and subclustering analysis was performed to identify major cell types and subpopulations. Malignant cells were identified by copy number variation analysis using inferCNV. Analysis details can be found in Supplementary material.

Results
To understand the role of the TIME in PSCC, scRNA-seq (10×Genomics) was performed (Fig. 1A). We prospectively collected 10 fresh tumor specimens with 6 HPV positive from penile, lymph node and distant metastatic sites with pathologically confirmed PSCC at localized (n = 3) and advanced (n = 7) stages, detailed clinicodemographic information may be found in Supplementary Table 1. 36,903 cells were retained after quality control (Supplementary Fig. 1A,B). 17 major cell types were identified based on canonical marker genes (Fig. 1B,C, Supplementary Fig. 1C,D, Methods). All cell clusters were present in all samples although
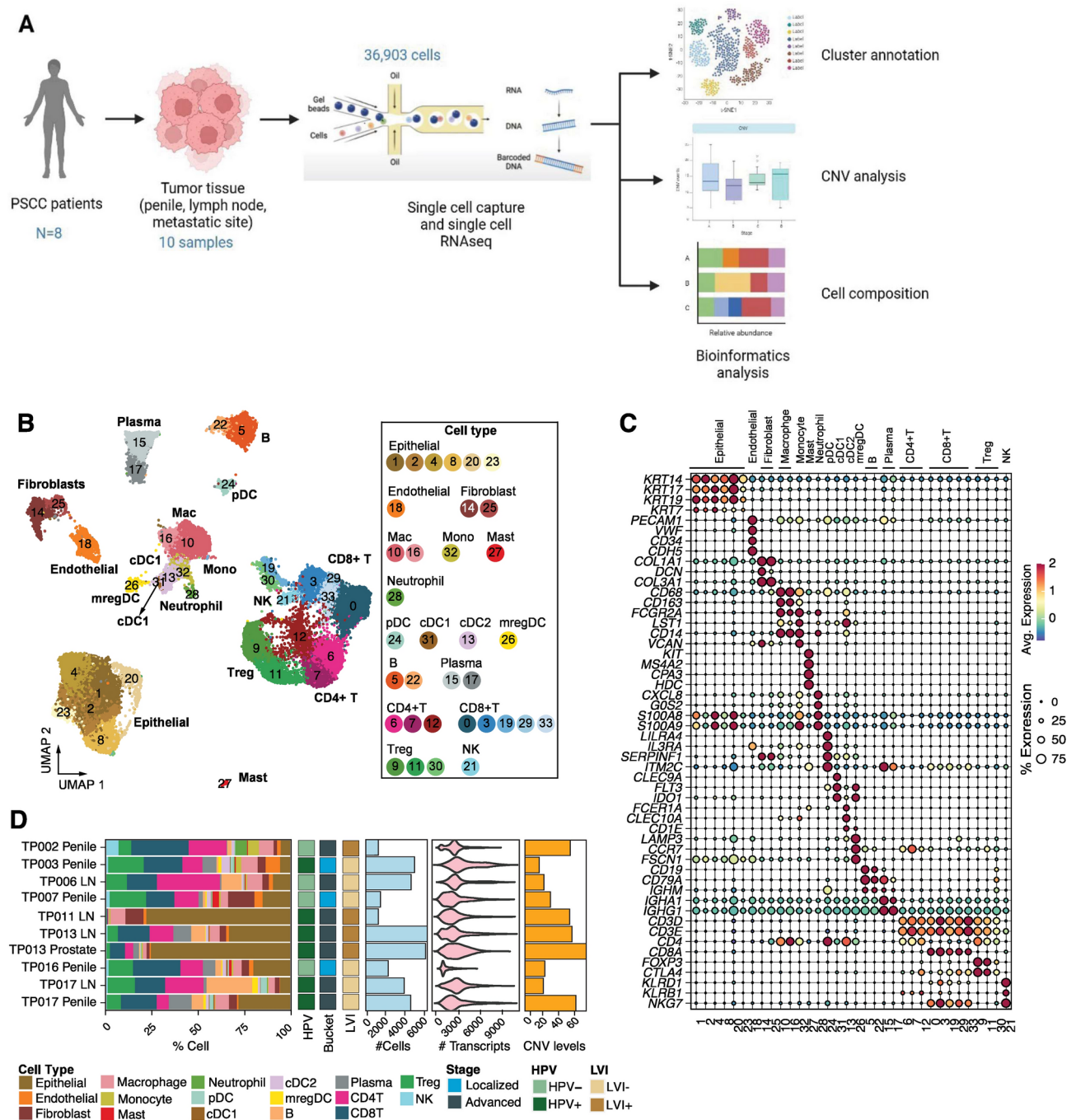
Fig. 1. Single-cell profiling of PSCC. (**A**) Overall flow chart of study. Fresh tissue obtained from surgery. Workflow incorporates single-cell dissociation, single-cell isolation, library construction, and sequencing. Raw data output is normalized and corrected prior to downstream analysis. (**B**) UMAP plot showing 34 clusters and 17 major cell types. (**C**) Dot plot showing representative marker genes across cell clusters. Dot size is proportional to the fraction of cells expressing specific genes with color intensity corresponding to the relative expression of specific genes. (**D**) Visual representation of major cell type composition, clinicodemographic variables and CNV levels per sample. Bucket, localized (bucket 1) and advanced disease states (bucket 2/3); LVI: lymphovascular invasion.

the epithelial and immune cells were enriched in specimens from lymph node and distant metastatic sites in comparison to penile samples (Fig. 1D). We specifically compared across advancing disease stage where epithelial, CD4$^+$ T cells and B cells were enriched in advanced stages in comparison to localized stage, where on the other hand endothelial cells, mast cells, dendritic cells and T regulatory cells were enriched in localized disease in comparison to advanced stage (Supplementary Fig. 1E). When compared by HPV status CD8$^+$, CD4$^+$

T cells and T regulatory cells were more enriched in HPV negative in comparison to HPV positive samples (Supplementary Fig. 1F).

Copy number variation (CNV)

To define malignant PSCC cells from benign cells, CNV was estimated from gene expression using inferCNV (Supplementary Fig. 2A,B, Methods). We inferred the single-cell CNV profile in PSCC epithelial cells using endothelial cells and fibroblast cells as a control. Within each patient, epithelial cells were clustered into clones based on their CNV status. Amplification of 1q, 3q, 17q and deletion of 11q, 13q were most commonly seen in our cohort (Fig. 2A). In patients with matched tumor samples (TP013 and TP017), similar CNV patterns were seen suggesting a clonal lineage between the matched tumor samples.

Epithelial cells were then divided into three groups (low, medium, high) based on CNV level (Fig. 2B, Supplementary Fig. 2C,D). Localized disease stage was found to have a higher proportion of cells with low CNV burden while advanced disease states were found to have a higher proportion of cells with medium/high CNV burden (Fig. 2C). Epithelial cells from HPV + tumors were also found to have a higher proportion of medium/high CNV burden compared to HPV – tumors (Fig. 2D). These suggest increased genomic instability within advanced stage and HPV + PSCC.

We then compared the transcriptome among epithelial cells based on CNV burden (Fig. 2E). CNV low, medium, high and normal cells exhibited distinct differences in gene expression patterns. For example, a specific set of genes was expressed in CNV high epithelial cells including KRT15, PIK3R1, COL7A1, PITX2 and TFC2P2L1. Pathway enrichment with gene set enrichment analysis (GSEA) demonstrated upregulation of nearly all pathways including development, immune, metabolic, proliferation and signaling pathways in the CNV high group (Fig. 2F). In comparison, cells with low CNV burden did not show enrichment of these biological pathways.

Meta-programs reveal a hypoxia signature in advanced stage PSCC and HPV-positive PSCC

We next explored how gene expression states varied among malignant cells. We identified 11 clusters from epithelial cells (Fig. 3A, Supplementary Fig. 3A and B) and mapped them to meta-programs to assess the diverse cellular pathways, identifying specific cluster association MP families, mainly cluster 8 with hypoxia, cluster 0 and 2 with cell cycle and cluster 11 with stress (Fig. 3B)[16]. We identified significant enrichment in hypoxia-related genes exclusively in samples from lymph node and distant visceral metastatic tumor sites in comparison to primary penile tumor tissue (Fig. 3B, Supplementary Fig. 3C).

GSEA revealed differential pathways in localized versus advanced disease as well as differences based on HPV infection status (Fig. 3C). Localized disease states and HPV – tumors were enriched for cell cycle genes and upregulation of E2F, or cell proliferation signaling. Advanced disease states and HPV + tumors were enriched for hypoxia-related genes and upregulation of MYC, KRAS and TNFα signaling (Fig. 3D,E). Recent effort in Glioblastoma has identified hypoxia related cues to induce hypoxia-related TAM associated with advanced stage and potential TAM targeted therapies[14]. Since such association has not been determined for PSCC we next assessed the cellular immune landscape in PSCC concurrent with this hypoxic signature in advanced stage.

Increased exhausted T cell and hypoxia M2 macrophage concurrent with decrease in effector T regulatory cells in advanced PSCC

To understand the transcriptional heterogeneity within tumor-infiltrating immune cells, we identified sub populations through subclustering and differential gene expression analysis (Methods). 11 individual T cell populations were identified, including regulatory T cells (Treg), CD4 + naïve T cells (Tn), exhausted CD8 + T cells (Texh) (Fig. 4A–C, Supplementary Fig. 4A,B). Similarly, nine individual myeloid cell populations were identified including tumor associated macrophages (TAMs), dendritic cells (DC), neutrophils, monocytes, and mast cells (Fig. 5A,B, Supplementary Fig. 5A).

To explore the hypothesis that there is progressive immune dysfunction with advancing disease stage, we compared lymphoid and myeloid cell populations in localized tumor samples to advanced disease state tumor samples. In advanced stage disease, an increase in CD4$^+$ Tn cells and CD8$^+$ Texh is seen with a decrease in effector Tregs (TNFRSF9 + Treg)[17,18] and naïve Treg cells (TNFRSF9 – Treg) which were noted to be quiescent (Fig. 4D,E, Supplementary Fig. 4C,D). This represents the inability of Texh to activate naïve T cells. We compared macrophages from advanced disease state tumors to those from earlier stages and found an increase in aging hypoxia associated TAM (LA-TAM) that correlated with the M2-like immunosuppressive TAM population in advanced/metastatic tumors (Fig. 5C,D, Supplementary Fig. 5C,D). Presence of M2-like TAMs are associated with T cell response suppression. These macrophages were found to have higher MYC and phosphorylation signature expression associated with aging hypoxic TAMs[19,20](Supplementary Fig. 5A). Overall, these data suggest an increased presence of M2-like immunosuppressive macrophages and exhausted T cells with significant decrease in effector Treg cells in advanced disease. This immune composition phenotype has been associated with resistance to PD-1 and PDL-1 immune checkpoint blockade (ICB) in other cancers and would present the explanation for the reported low response rates to PD-1 ICB for advanced PSCC in comparison to other cancers like melanoma or RCC[21].

Increase in immunosuppressive Treg subsets CD8 T cell exhaustion with increase in hypoxia M2 TAMs in HPV associated PSCC

Cluster classification analysis was performed from scRNA-seq data and the abundance of various T cell and myeloid cell types between HPV + and HPV – samples were noted. Compared to HPV – PSCC, HPV + tumors displayed increased infiltration of LA-TAM aging M2 macrophages (Fig. 5B–D), effector TNFRSF9 + Tregs and Texh consistent with an anti-viral response (Supplementary Fig. 5A).
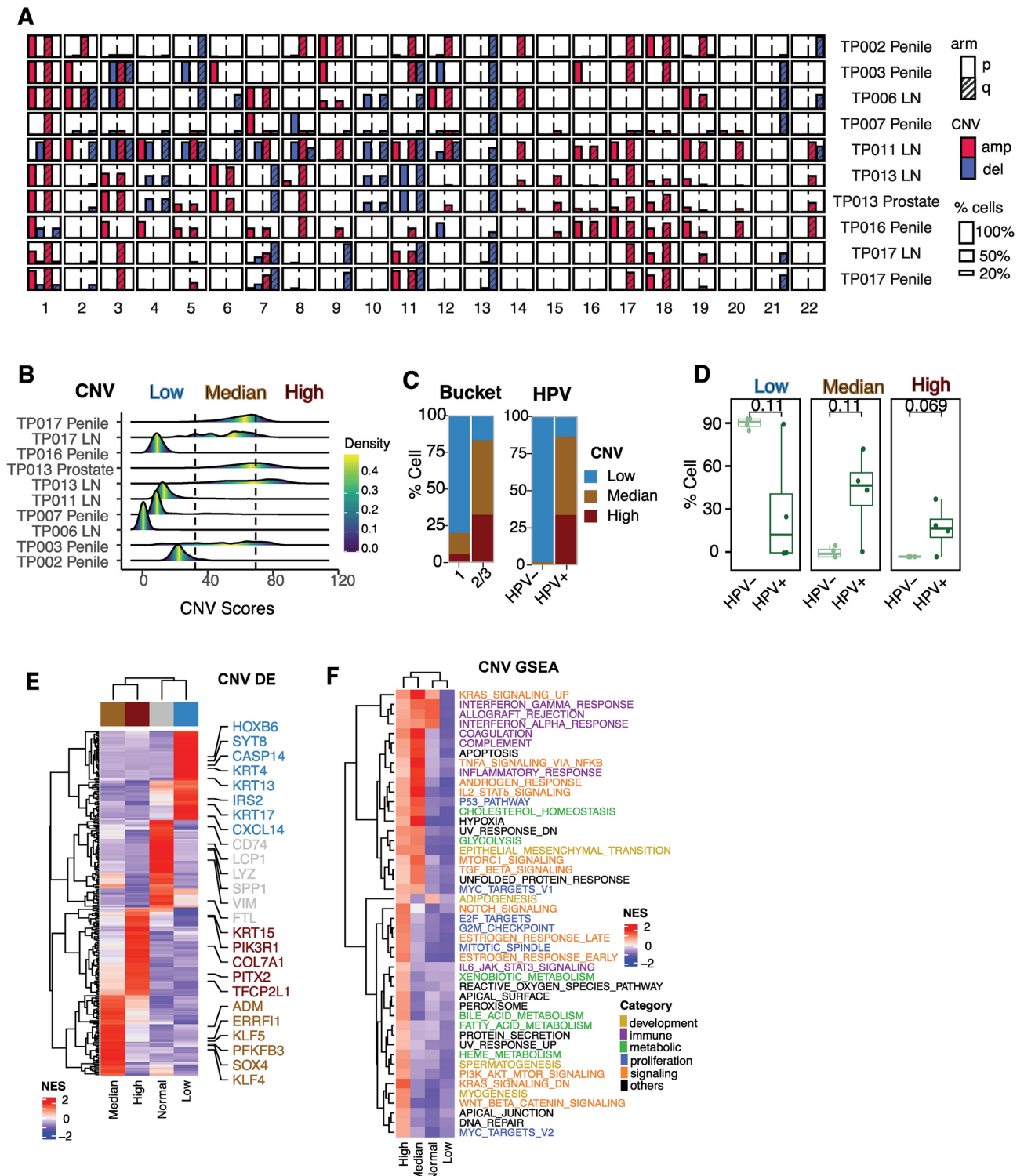
Fig. 2. (**A**) Copy number variation (CNV) differences by sample. Amplification of 1q, 3q, 17q and deletion of 11q, 13q most commonly seen. (**B**) CNV stratified by low, medium and high per sample. Ridgetplot shows the distribution of CNV scores in different samples. Dash line represents the threshold. Color shows the density of distribution. (**C**) Proportion of tumor cells with low, medium and high CNV by bucket and HPV status (**D**) Box plot demonstrating proportion of tumor cells with low, medium and high CNV stratified by HPV status). *P*-value was calculated by two-sided Wilcoxon rank-sum test. Box plot shows the median (central line), the 25% and 75% interquartile (IQR) (lower and upper hinges), the ± 1.5 IQR (Tukey whiskers), and all data points. (**E**) Heatmap of differentially expressed genes across different CNV status and normal epithelial cells. Shown are Z-scored gene expression values. (**F**). GSEA analysis of Hallmark gene sets across different CNV status and normal epithelial cells. Shown are normalized enrichment scores. Hallmark gene sets were colored by categories.
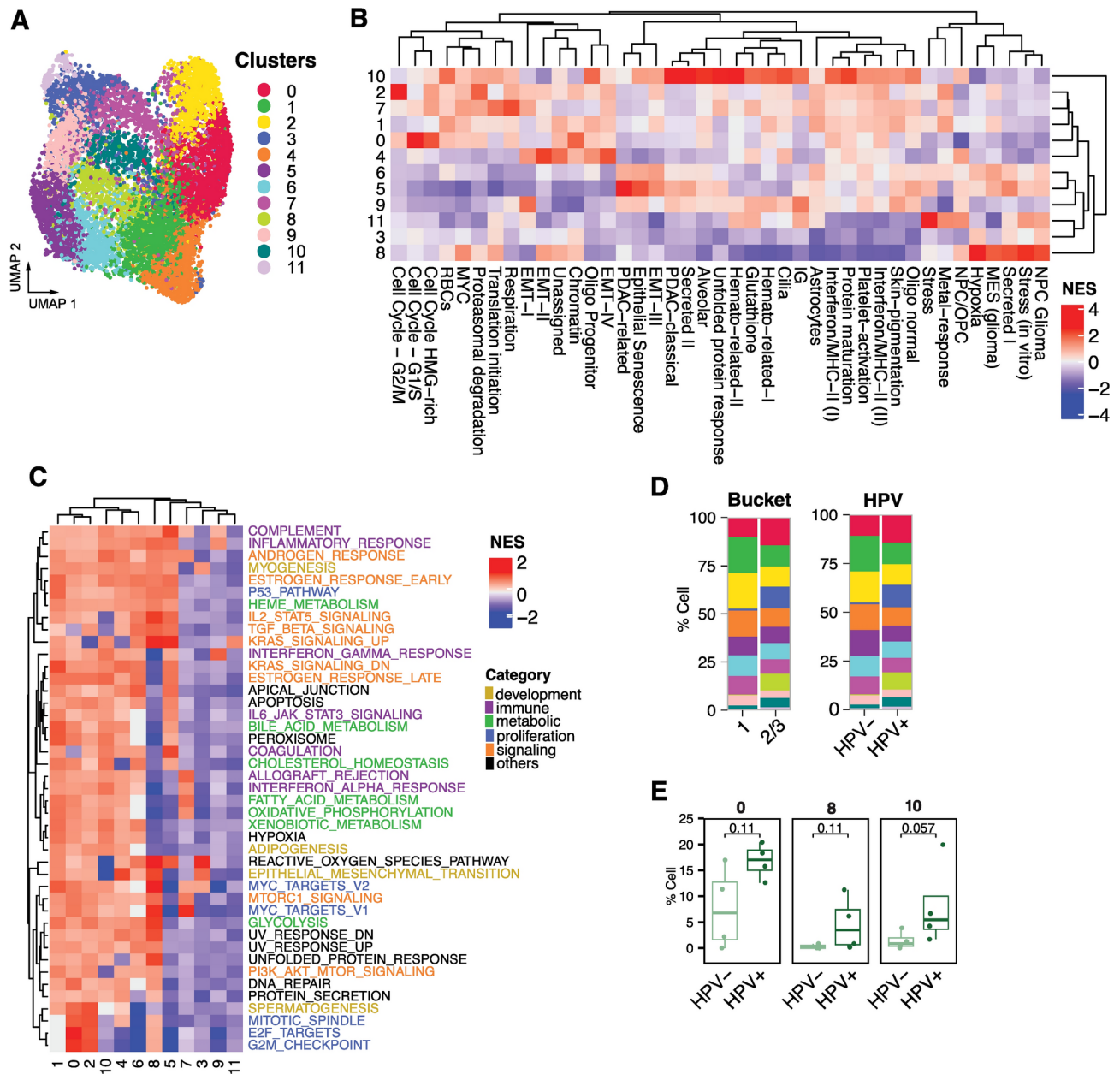
Fig. 3. Epithelial cells. (**A**) 12 clusters identified from epithelial cells. (**B**) GSEA analysis of cancer meta-programs indicating transcriptional intratumour heterogeneity. Shown are normalized enrichment scores of each program. (**C**) GSEA analysis of Hallmark gene sets across 12 epithelial clusters Shown are normalized enrichment scores. Hallmark gene sets were colored by categories. (**D**) Cluster composition by bucket and HPV status. (**E**) Box plot demonstrating increase in cluster 0, 8, 10 cells seen in HPV positive patients. *P*-value was calculated by two-sided Wilcoxon rank-sum test. Box plot shows the median (central line), the 25% and 75% interquartile (IQR) (lower and upper hinges), the ± 1.5 IQR (Tukey whiskers), and all data points.

Discussion

Building on the first single-cell transcriptomic effort this study provides a single-cell atlas of the PSCC tumor and immune landscape, dissecting the distinct immune cell populations and transcriptional profiles with advancing disease stage across tumor sites from penile, lymph node and visceral metastatic sites. These insights into the PSCC immune landscape offer a foundation for identifying and optimizing targeted immunotherapeutic approaches. Our findings suggest that tumor progression and HPV status significantly shape the immune microenvironment in PSCC, identifying the novel role TNSF9 T reg cells, exhausted Cd8T cells and enrichment in aging M2 TAMs in PSCC immune evasion mechanisms that contribute to disease progression. To date, the immune microenvironment of PSCC across advancing disease states remains poorly characterized at the single-cell level. Our work presents the first scRNA-seq atlas in PSCC to cover differences across progressive disease states. Localized PSCC were noted to have a dynamic immune phenotype with an active innate immune system
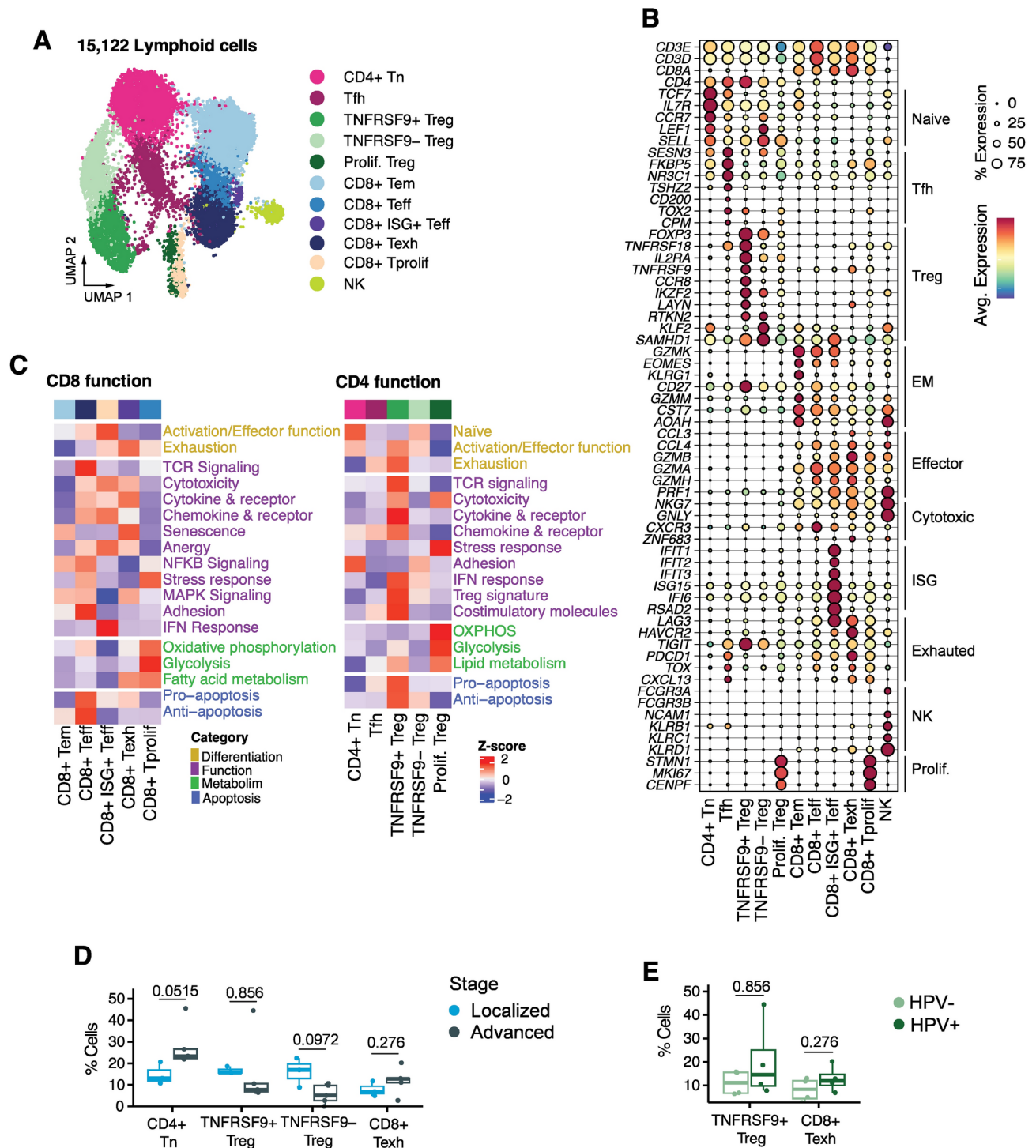
Fig. 4. Lymphoid cells. (**A**) UMAP of T and NK cell subtypes. (**B**) Dot plot of canonical and functional markers for individual T and NK cell populations. Dot size is proportional to the fraction of cells expressing specific genes with color intensity corresponding to the relative expression of specific genes. (**C**) Signatures scores of 16 curated gene sets related to CD8 + and CD4 + T cell functional states across T cell subpopulations. Shown are z-score normalized signature scores. Gene sets are colored by categories. (**D**) Box plot of differences in CD4 + naïve T cell, regulatory T cell (TNFRSF9 + and TNFRSF9 − Treg) and CD8 + exhausted T cell populations between bucket 1 and 2/3. (**E**) Box plot representing differences in regulatory T cell and Cd8 + exhausted T cell populations between HPV status. *P*-value was calculated by two-sided Wilcoxon rank-sum test. Box plot shows the median (central line), the 25% and 75% interquartile (IQR) (lower and upper hinges), the ± 1.5 IQR (Tukey whiskers), and all data points.
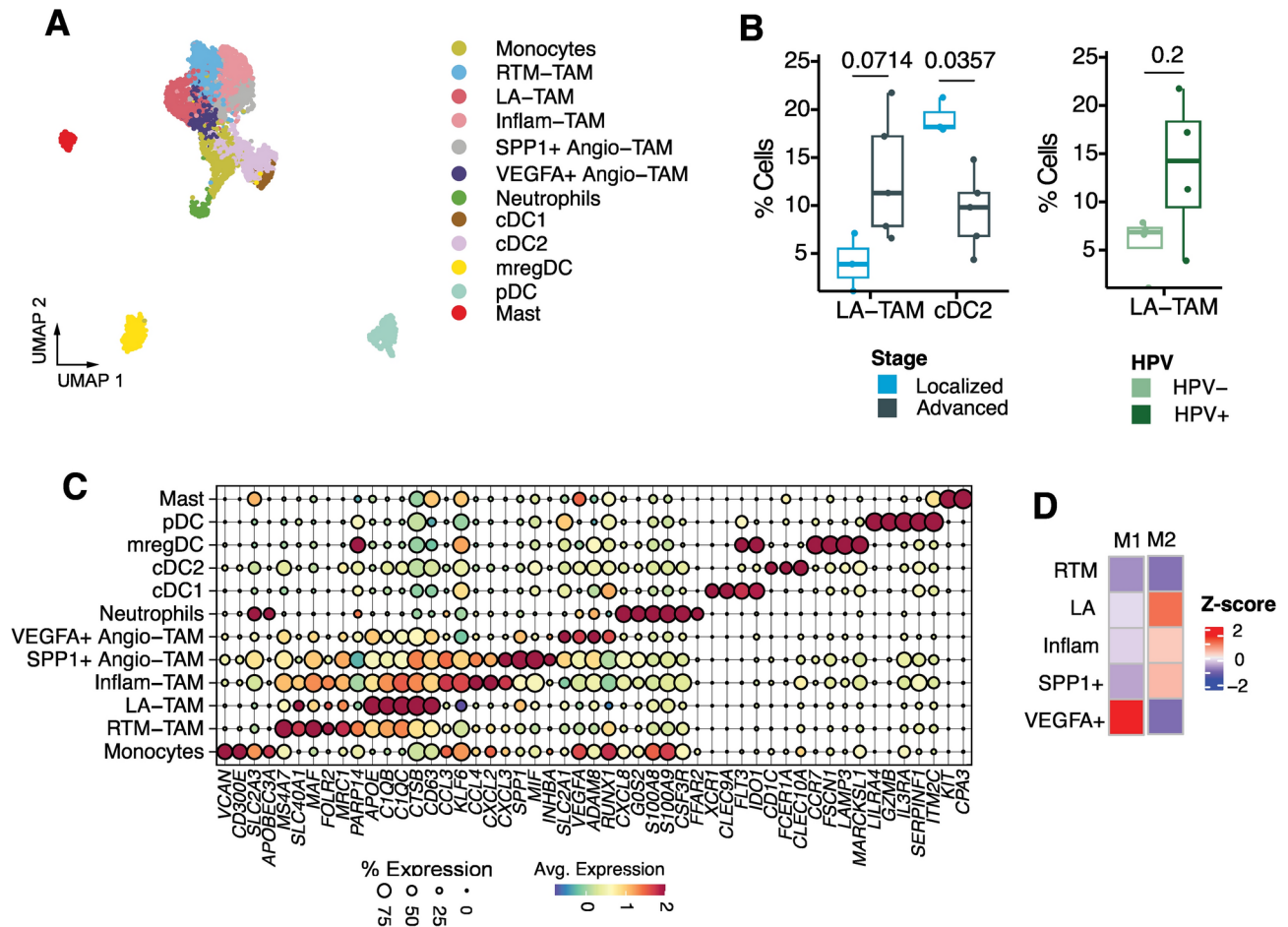
Fig. 5. Myeloid cells. (**A**) UMAP of myeloid subtypes including macrophages, monocytes, neutrophils, dendritic cells, and mast cells. TAM, tumor associated macrophages; Angio, pro-angiogenic; Inflam, inflammatory cytokine-enriched; LA, lipid-associated; RTM, resident tissue macrophages, mregDC, mature immunoregulatory dendritic cells. (**B**) Box plot representing differences in LA-TAM and cDC2 populations in bucket 1 versus 2/3 and HPV status. *P*-value was calculated by two-sided Wilcoxon rank-sum test. Box plot shows the median (central line), the 25% and 75% interquartile (IQR) (lower and upper hinges), the ± 1.5 IQR (Tukey whiskers), and all data points. (**C**) Bubble plot of canonical and functional markers provides phenotypic information for individual myeloid cell populations. (**D**) M1/M2 score for various TAMs. See M1 and M2 signatures in Supplementary Table 2.

characterized by increased DC, alongside signs of early immunosuppression evidenced by increased Tregs. Alternatively, advanced disease are characterized by an increase in aging pro-tumor M2-type macrophages with increased Texh and inactive, Tn cells suggestive of a supportive microenvironment for tumor growth. The changes seen from localized to advanced disease states suggests a failure of tumor clearance and the development of immune evasion mechanisms to allow progression and metastasis of the tumor. T cell exhaustion is a major obstacle in cancer immunotherapy as it limits the effectiveness of T cells in eliminating tumor cells. Exhausted T cells exhibit a dysfunctional phenotype characterized by the upregulation of inhibitory receptors like PD-1 and PD-L1. Use of immune checkpoint inhibitors can overcome T cell exhaustion by blocking the inhibitory receptors on exhausted T cells, allowing them to regain their anti-tumor activity. Presence of M2-like macrophages also create pro-tumor environments through high expression of immune checkpoint molecules (PD-L1) resulting in T cell exhaustion[5,22]. The increase in presence of M2-like macrophages in advanced PSCC have been corroborated in multiplex immunofluorescence studies comparing early to advanced stage PSCC. Detailed scRNA-seq analysis revealed a shift in transcriptional hallmarks from cell cycle with upregulation of proliferative, E2F signaling in localized disease to tumor hypoxia with upregulation of cell proliferation and angiogenesis signaling in advanced disease. This hypoxic tumor environment is known to promote pro-tumorigenic M2 polarization of TAMs, aligning with our findings of increased aging M2 TAMs in advanced PSCC. The observed enrichment of aging M2 TAMs and CD8 + Texh are thought to create an immunosuppressive TME through inhibition of T cell activation and may contribute to the limited efficacy of PD-1 immune checkpoint inhibitors in this advanced disease setting. Integrating meta-programs and Hallmark GSEA into scRNA-seq data analysis revealed key biological pathways and processes associated with HPV status. HPV – tumors demonstrated a cell cycle hallmark with upregulation of cell proliferation signaling. These tumors were also noted to have cells with

lower CNV compared to HPV + tumors. Alternatively, HPV + tumors were found to have a hypoxia hallmark with upregulation of cell proliferation and angiogenesis signaling. Tumor hypoxia is traditionally a hallmark associated with more aggressive tumors and results in T cell dysfunction to exhausted CD8 T cells which was noted in the immune microenvironment of HPV + tumors in our cohort[23]. Although multiple factors contribute to T cell exhaustion, the combination of persistent antigen stimulation from the HPV virus and tumor hypoxia are likely driving the T cell exhaustion immune phenotype. Furthermore, the higher CNV seen in HPV + tumors suggest a potential benefit from ICB therapy.

While the immune landscapes of HPV + and HPV – tumors remain incompletely understood, Rafael et al. found that presence of M2-type macrophages in the TME of HPV + patients was significantly associated with increased tumor grade and lymph node metastasis[14]. Our results validate this finding with increased presence of M2-like TAMs both in advanced stage and HPV + tumors. Our single cell work demonstrates a deficiency in tumor infiltrating lymphocytes (TILs) in HPV – tumors. These "immune-excluded" tumors have previously been associated with advanced T stage, lymph node metastasis and poor prognosis, with limited response to single-agent ICB[24,25]. Thus, patients with immune-excluded tumors are in need of novel therapies to improve outcomes. In comparison, HPV + tumors exhibited greater immune infiltration characterized by increased DCs, M2- like macrophages, Tregs and Texh. This phenomenon of immune cell infiltration into the tumor termed "immune-inflamed" leads to an immune exhausted phenotype, where T cells are unable to effectively eliminate tumor cells[24]. The presence of M2-like macrophages further contributes to immunosuppression by promoting a tumor-supportive environment. This immune exhausted phenotype observed in HPV + tumors suggest that these tumors may be responsive to ICB. However, further research with a larger cohort is needed to definitively elucidate the mechanism by which HPV infection shapes the TIME, its predictive value for immunotherapy response, and the role of immunosuppressive lymphocytes and Texh in PSCC prognosis.

Several limitations exist in the present study. Firstly, the relatively small sample size of 10 PSCC samples, derived from a single center, may limit the generalizability of our findings. Nevertheless, to our knowledge this is the first study to include samples not only from primary penile tumors but from lymph node and distant metastatic tumor sites, offering a unique ability to provide valuable insight into changes in the immune cell population across advancing disease stages. Secondly, the snapshot nature of scRNA-seq limits our ability to fully capture the complex temporal and spatial dynamics of immune cell infiltration. Without concurrent spatial transcriptomics data, we cannot account for intratumoral heterogeneity, which may influence the observed immune cell profiles. Finally, while scRNA-seq enables the identification of distinct cell populations and their associated gene expression patterns, linking these patterns to functional outcomes remains a significant challenge. In the absence of validation studies, it can be difficult to definitively interpret the biological significance of these findings. Additionally, technical limitations inherent to scRNA-seq including batch effects and potential cell loss during sample preparation may introduce noise into the data analysis.

Conclusion

In this study, we describe the differences in the TIME and transcriptional hallmarks using scRNA-seq data across advancing disease states and HPV status. Our analysis reveals a TIME of progressive T cell exhaustion and pro-tumor aging TAMs seen in advanced disease identifying mechanisms of immune evasion. HPV status showed a difference in immune cell infiltration into the TIME with HPV – tumors showing an immune-excluded phenotype and HPV + tumors showing an immune-inflamed, but exhausted phenotype. These findings add to the growing knowledge of the TIME in PSCC and allow us to gain insight into potential therapeutic strategies for advanced PSCC.

Data availability

Processed single-cell RNAseq data are available on request from the corresponding authors.

References
1. Key Statistics for Bladder Cancer. https://www.cancer.org/cancer/types/bladder-cancer/about/key-statistics.html Accessed March 12, 2024.
2. Joshi, V. B., Spiess, P. E., Necchi, A., Pettaway, C. A. & Chahoud, J. Immune-based therapies in penile cancer. *Nat. Rev. Urol.* **19**, 457–474 (2022).
3. Chahoud, J. et al. Prognostic significance of p16 and its relationship with human papillomavirus status in patients with penile squamous cell carcinoma: Results of 5 years follow-up. *Cancers* **14**, 6024 (2022).
4. Parza, K. et al. The prognostic role of human papillomavirus and p16 status in penile squamous cell carcinoma-a systematic review. *Cancers* **15**, 3713 (2023).
5. Ionescu, F. et al. Multiplex immunofluorescence captures progressive immune exhaustion with advancing penile squamous cell cancer stage. *Cancers* **16**, 303 (2024).
6. Thomas, A. et al. Establishment, characterization, and imaging of a first platinum-resistant penile cancer patient-derived xenograft in nude mice: A eUROGEN project. *Eur. Urol.* **78**, 294–296 (2020).
7. Binnewies, M. et al. Understanding the tumor immune microenvironment (TIME) for effective therapy. *Nat. Med.* **24**, 541–550 (2018).
8. Nofech-Mozes, I., Soave, D., Awadalla, P. & Abelson, S. Pan-cancer classification of single cells in the tumour microenvironment. *Nat. Commun.* **14**, 1615 (2023).
9. Elst, L. et al. Single-cell atlas of penile cancer reveals TP53 mutations as a driver of an aggressive phenotype, irrespective of human papillomavirus status, and provides clues for treatment personalization. *Eur. Urol.* **86**, 114–127 (2024).
10. Chahoud, J., Xiaoqing, Y., Necchi, A. & Spiess, P. E. TP53 mutations emerge as a critical biomarker in penile cancer, superseding human papillomavirus status. *Eur. Urol.* **86**(2), 128–129. https://doi.org/10.1016/j.eururo.2024.04.032 (2024).

11. Zhang, L. et al. Single-cell analyses inform mechanisms of myeloid-targeted therapies in colon cancer. *Cell* **181**, 442-459.e429 (2020).
12. Zhang, L. et al. Lineage tracking reveals dynamic relationships of T cells in colorectal cancer. *Nature* **564**, 268–272 (2018).
13. Zheng, C. et al. Landscape of infiltrating t cells in liver cancer revealed by single-cell sequencing. *Cell* **169**, 1342-1356.e1316 (2017).
14. Wang, W. et al. Identification of hypoxic macrophages in glioblastoma with therapeutic potential for vasculature normalization. *Cancer Cell* **42**, 815-832.e812 (2024).
15. Braun, D. A. et al. Progressive immune dysfunction with advancing disease stage in renal cell carcinoma. *Cancer Cell* **39**, 632-648.e638 (2021).
16. Gavish, A. et al. Hallmarks of transcriptional intratumour heterogeneity across a thousand tumours. *Nature* **618**, 598–606 (2023).
17. Li, Y. et al. Tumor-infiltrating TNFRSF9(+) CD8(+) T cells define different subsets of clear cell renal cell carcinoma with prognosis and immunotherapeutic response. *Oncoimmunology* **9**, 1838141 (2020).
18. Cho, J. W., Son, J., Ha, S. J. & Lee, I. Systems biology analysis identifies TNFRSF9 as a functional marker of tumor-infiltrating regulatory T-cell enabling clinical outcome prediction in lung cancer. *Comput. Struct. Biotechnol. J.* **19**, 860–868 (2021).
19. Moss, C. E. et al. Aging-related defects in macrophage function are driven by MYC and USF1 transcriptional programs. *Cell Rep.* **43**, 114073 (2024).
20. Wculek, S. K. et al. Oxidative phosphorylation selectively orchestrates tissue macrophage homeostasis. *Immunity* **56**, 516-530.e519 (2023).
21. El Zarif, T. et al. Safety and efficacy of immune checkpoint inhibitors in advanced penile cancer: Report from the Global Society of Rare Genitourinary Tumors. *J. Natl. Cancer Inst.* **115**, 1605–1615 (2023).
22. Ma, R. Y., Black, A. & Qian, B. Z. Macrophage diversity in cancer revisited in the era of single-cell omics. *Trends Immunol.* **43**, 546–563 (2022).
23. Bannoud, N. et al. Hypoxia supports differentiation of terminally exhausted CD8 T cells. *Front. Immunol.* **12**, 660944 (2021).
24. Tiwari, A. et al. Towards a consensus definition of immune exclusion in cancer. *Front. Immunol.* **14**, 1084887 (2023).
25. Chu, C. et al. Immunophenotypes based on the tumor immune microenvironment allow for unsupervised penile cancer patient stratification. *Cancers* **12**, 1796 (2020).

Acknowledgements

Author contributions

Jad Chahoud and Philippe Spiess had full access to all the data in the study and takes responsibility for the integrity of the data and the accuracy of the data analysis. Study concept and design: Chahoud and Spiess Acquisition of data: Le, Miyagi, Chahoud, Peak, Spiess Analysis and interpretation of data: Miyagi, Yu, Chahoud Drafting of manuscript: Miyagi, Yu, Chahoud Critical revision of the manuscript for important intellectual content: All authors. Statistical analysis: X. Yu Obtaining fundings: Chahoud Administrative, technical, or material support: Yoder, Marchion, Zhang. Supervision: Chahoud, Spiess.

Declarations

Competing interests

P E Spiess reports the following leadership positions: President of Global Society of Rare GU Tumors, NCCN bladder and penile cancer panel, vice-chair, Member of ASCO/EAU Penile Cancer Panel. J Chahoud received consultation fees from Pfizer, Aveo, Eisai, Merck, Exelixis and mycaregorythm. The authors have no other relevant affiliations or financial involvement with any organization or entity with a financial interest in or financial conflict with the subject matter or materials discussed in the manuscript apart from those disclosed.

Additional information

Supplementary Information The online version contains supplementary material available at https://doi.org/10.1038/s41598-025-89760-0.

Correspondence and requests for materials should be addressed to H.M. or J.C.

Reprints and permissions information is available at www.nature.com/reprints.

Publisher's note Springer Nature remains neutral with regard to jurisdictional claims in published maps and institutional affiliations.